Thermal magnetic properties of the Ni sublattice in half-metallic NiMnSb: A theoretical study based on first-principles calculations

L. M. Sandratskii*
Max-Planck-Institut für Mikrostrukturphysik, Weinberg 2, D-06120 Halle, Germany
(Received 12 June 2008; revised manuscript received 2 September 2008; published 30 September 2008)

We report a detailed theoretical study of the thermal magnetic properties of the Ni sublattice in half-metallic NiMnSb. The study is performed in the temperature interval where the disordering of the Mn sublattice is weak and the properties of the Ni sublattice can play a crucial role. In earlier work it was suggested that the behavior of the Ni sublattice is responsible for the anomalies in the properties of NiMnSb detected experimentally at about 80 K. Because of high Curie temperature T_C=730 K the interval of weak Mn disorder extends up to the technologically important room temperature. We formulate a thermodynamic model where both transversal and longitudinal fluctuations of the magnetic moments are taken into account. The energies of the fluctuations are determined by means of the constrained calculations within the framework of density-functional theory. We show that the half-metallicity is robust with respect to the longitudinal atomic fluctuations in the ground-state ferromagnetic structure. On the other hand the half-metallicity imposes strong restrictions on the longitudinal fluctuations. In contrast to longitudinal fluctuations the transversal fluctuations disturb the half-metallicity. We show that the contributions of the longitudinal and transversal fluctuations to the temperature dependence of the Ni net magnetization compensate, which leads to a very weak variation of the Ni magnetization in a broad temperature interval. This feature is in agreement with experiment. Simultaneously a large amplitude of the fluctuations results in strong decrease in the spin polarization of the Ni DOS at the Fermi level. The calculated temperature dependence of the Ni spin polarization reveals a crossover in the temperature interval between 75 and 100 K that correlates with experimental features in the temperature dependences of the physical properties. Although this crossover cannot be interpreted as the transition from a half-metallic to a non-half-metallic state the half-metallicity of the ground state is an important factor determining the properties of the fluctuations and the temperature properties.

DOI: 10.1103/PhysRevB.78.094425 PACS number(s): 75.50.Cc, 75.30.Et, 71.15.Mb

I. INTRODUCTION

The ferromagnetic Heusler compound NiMnSb is a prototype half-metallic system.[1] In the ferromagnetic ground state the electron structure of the majority-spin channel is metallic whereas the minority-spin electron structure is semiconducting. The half-metallicity leads to a high spin polarization of the charge carriers that makes possible an efficient injection of the spin-polarized current into semiconductors. This feature is crucial for materials suitable for applications in spintronic devices utilizing both the charge and the spin of electrons. The half-metallic materials are currently the object of intensive researches. (See Ref. 2 for a recent detailed review on different aspects of the physics of half-metallic systems.)

Since the devices must be operative at room temperature it is important to understand the finite-temperature processes in the half-metallic systems. A number of experimental researches revealed the presence of the anomalies in the physical properties at temperature of about 80 K.[3,4] These anomalies were attributed to a transition from half-metallic to normal metallic state. There are, however, a number of aspects that make an assumption of such a transition questionable. First, in an exact mathematical sense the half-metallicity is destroyed at any nonzero temperature. Indeed, a certain magnetic disorder is present at any temperature above 0 K. Therefore a snap-short of the magnetic configuration at a nonzero temperature is a noncollinear magnetic structure. In noncollinear magnets the electron spin projection is not a good quantum number. Therefore each electron wave function has both spin components and the spin polarization does not reach the value of 100%.

The assumption used in the interpretation of the experimental anomalies that the half-metallicity disappears first above a certain critical temperature T_{cr} is based on the Stoner picture of the thermodynamics of itinerant magnets. This picture neglects the disordering of atomic moments. The influence of temperature appears here as the consequence of the smoothing of the Fermi-Dirac distribution function. The Stoner picture preserves at any temperature the collinear ferromagnetic structure and therefore the spin projection as a good quantum number. However, this picture fails to give a reasonable estimation of the Curie temperature of magnets and cannot explain a typical Curie-Weiss form of the paramagnetic susceptibility. It is commonly considered as insufficient for the description of the thermal properties of magnets. Within the Stoner picture the change in the electron structure of NiMnSb at 80 K is negligibly small compared to the energy of the half-metallic gap and cannot lead to the disappearance of the half-metallicity.

On the other hand, if we now take the spin disordering into account and try to relate the anomalies at 80 K to quantitative changes in the spin polarization we will see that also in this way the relation is not straightforward. Indeed the Curie temperature of NiMnSb T_C=730 K is high and at 80 K the experimental magnetization is still 99.5% of the ground-state value.[3,5] In terms of the rotation of rigid atomic moments this corresponds to the deviation of the moments

from the z axis by an angle of 5.73°. The atomic states whose spin orientation is rotated together with the atomic moment give the 99.5% spin polarization with respect to the global z axis and no spectacular quantitative changes in the electronic structure can be expected. Even at room temperature the experimental decrease in the magnetization is of 8% only.[3,5] The picture of the rotated rigid atomic moments gives high value of 92% for the spin polarization of the charge carriers.

Since the Mn sublattice cannot be noticeably disordered at 80 K the reason for the anomalies was assumed to be in the thermal collapse or strong disorder of the Ni magnetic moments.[4,6,7] Ležaić *et al.* have shown that under certain model assumptions a strong drop of the Ni magnetization can be obtained already at 50 K. This drop of the Ni magnetization is, however, directly reflected in the calculated total magnetization as a corresponding decrease as a function of temperature.[6] In contrast, the experimental magnetization curve does not have any noticeable features in this temperature region.[3,5]

The purpose of this paper is to study in detail the thermodynamics of the Ni sublattice in the temperature interval where the disorder of the Mn moments is weak. The thermal properties of the Ni sublattice are related to the spin polarization of the states at the Fermi level. Special attention is devoted to the account for the longitudinal fluctuations of the Ni moments. In particular the restrictions on the longitudinal fluctuations imposed by the half-metallicity are addressed. The considerations performed in the paper are of rather general character and may be useful in the studies of various multiple-sublattice systems, in particular, various half-metallic systems.

The paper is organized as follows: In Sec. II we describe the first-principles approaches to the thermodynamics of the itinerant magnets. In Sec. III we present the calculations of the transversal and longitudinal fluctuations of the Ni moments. The restrictions on magnetic excitations imposed by half-metallicity are discussed. In Sec. IV we formulate the thermodynamic model and report the results of the calculations of the temperature dependences of magnetic properties.

II. FIRST-PRINCIPLES STUDY OF THE THERMODYNAMICS OF ITINERANT MAGNETS

A widely accepted approach to study the ground state of solids is density-functional theory (DFT). In principle, DFT can be extended to the consideration of the magnetic properties at finite temperatures.[8] The corresponding functional is however not known. As mentioned above in the early studies the thermodynamics of itinerant-electron magnets was considered to be governed by thermal smoothing of the Fermi-Dirac distribution function. This approach failed to describe the key magnetic properties.[9] The reason for the failures was understood in the neglect of the transversal magnetic fluctuations.

A convenient and most often used approach to introduce the transversal fluctuations into the itinerant-electron picture is based on a hypothesis that the magnetic excited states of the system can be uniquely characterized by specifying the directions of the atomic moments $\{\mathbf{e}_i\}$.[10] Here index i numbers the atoms. The constrained minimization of the energy as a functional of the electron density and magnetization allows the calculation of the electron properties of the state specified by $\{\mathbf{e}_i\}$.[11] The total energy as a function of the directions of the atomic moments $E(\{\mathbf{e}_i\})$ can be considered as model magnetic Hamiltonian of the system. The models where only the directions of the atomic moments are considered as independent variables are referred to in this paper as the Heisenberg-type models or **e** models. In the case where also the variation of the values of the atomic moments is included into consideration the models will be referred to as **m**-type models. For example the Ginzburg-Landau Hamiltonian used in the theory of magnetism can be considered as belonging to the **m**-type.[9]

Historically the mapping of itinerant-electron systems on the Heisenberg-type Hamiltonians was an important step in the understanding of the physics of magnetic materials. The thermodynamic properties of the Heisenberg Hamiltonian can be studied within different calculational approaches, e.g., mean-field approximation, random-phase approximation, and Monte Carlo simulation. Also the limitations of the mapping on the Heisenberg-type Hamiltonian become increasingly clear. For example, even for the elementary $3d$ metals like Fe and Ni the problem of the strength of the short-range magnetic order at and above T_C remains a topic of debate and was not solved within **e**-type models.[12,13] The investigations of more complex systems open additional questions. In our recent study of multiple-sublattice systems we have shown that the treatment on the same footing of the inducing and induced moments within the framework of the Heisenberg model leads to artificial features in the spin-wave spectrum.[14] Fortunately, these artificial features do not strongly influence the values of the Curie temperature estimated within both mean-field and random-phase approximations. In an alternative approach only the directions of the atomic moments of the inducing sublattice are considered as independent degrees of freedom whereas the magnetization of the atoms of the induced sublattice adjusts itself to the given configuration of the inducing moments. Within this treatment a substantial change in the estimated Curie temperature is obtained.

In the given paper we devote special attention to the role of the longitudinal fluctuations of the atomic moments. The possibility for the magnetization to vary in both the direction and the value is an essential feature of DFT. The ground state of the system is determined within DFT as an energy minimum with respect to such variations. As mentioned above the excited states of the system can be stabilized by means of the constrained minimization. In this way the states characterized by given values and directions of the atomic moments can be calculated.

The possibility to continuously change the value of the atomic moments in itinerant-electron magnets is closely related to the noninteger values of the atomic moments in such systems. The origin of the noninteger spin atomic moments is well understood. The hybridized atomic states form the bands of collective states extended over the system. These collective states are occupied by electrons according to the Fermi-Dirac distribution function. Although the number of the valence electrons per unit cell is an integer the number of the electrons with a given spin projection must not be an

integer. It depends on the energy dependence of the density of states (DOS), on the exchange splitting of the states, and on the position of the Fermi level. Also in half-metals the atomic moments remain noninteger. The moment per unit cell is, however, an integer that is the consequence of the semiconducting gap in one of the spin channels. Because of the gap all bands in this spin channel are either completely full or empty.

In accordance with the considerations given above two types of constrained calculations are performed. In the first type, only the directions of the atomic moments $\mathbf{e}_i$ are constrained whereas the values of the moments are determined in a self-consistent procedure supplying the state with the minimal total energy for the given configuration $\mathbf{e}_i$. The self-consistent values of the moments as a function of the magnetic configuration will be denoted as $m_i^0(\{\mathbf{e}_i\})$. The character of the dependence of the atomic moments on magnetic configuration is an important characteristic of the material. This dependence can be very different for different systems and even for different magnetic sublattices of the same system. If the value of the self-consistent moment depends weakly on the magnetic configuration the atomic moment is considered as robust and well defined. For example the Mn moment in NiMnSb depends weakly on the magnetic configuration.[14] Conceptually the case of robust atomic magnetic moments is best suited for the application of a Heisenberg-type Hamiltonian. If m_i^0 depends strongly on the magnetic configuration the concept of a robust atomic moment does not apply to atom i. The energy function $E(\{\mathbf{e}_i\})$ may still provide useful information on the thermodynamics of the system if the longitudinal stiffness of the magnetic moments is high and only the states with atomic moments close to m^0 give significant contribution to the average values. There is however an additional aspect consisting in the proper account for the statistical weight of the excited states in the case of strong dependence of m_i^0 on $\{\mathbf{e}_i\}$. These questions will be addressed below in Sec. IV.

In the second type of the constrained calculations not only the directions but also the values of the moments are constrained. The additional term to the energy functional responsible for the condition that the moment of the ith atom has a given value m has the following form:

$$h_i\left[\int_{\Omega_i} m(\mathbf{r})d\mathbf{r} - m_i\right], \tag{1}$$

where $m(\mathbf{r})$ is the projection of the magnetization on the direction $\mathbf{e}_i$. The integration is performed over the atomic sphere of the ith atom. After the variation of the energy functional, the Kohn-Sham equation contains an additional term corresponding to an external magnetic field $h_i\mathbf{e}_i$. The value of h_i is determined within a self-consistent procedure to give the magnetic moment m_i. Obviously, for a given magnetic configuration $\{\mathbf{e}_i\}$ the minimum of the total energy is given by the values of the magnetic moments equal to m_i^0. These states correspond to the zero constraining fields $h_i=0$.

III. MAGNETIC EXCITATIONS IN HALF-METALLIC NiMnSb

The half-metallicity imposes some restrictions on the magnetic excitations.[7] The spin-flip electron transitions between Bloch states have in half-metals an activation energy determined by the minimal distance between the Fermi level and the gap boundaries in the semiconducting channel. Therefore at the temperature of 80 K the probability of the thermally activated spin-flip transitions between Bloch states is very low. Because of the delocalized character of the Bloch states the change in the moment as a result of the spin-flip transition is equally distributed between the unit cells and gives very small effect on the value of the atomic moments.

On the other hand, the local longitudinal fluctuations of the atomic magnetization [Eq. (1)] that we consider in this paper do not have an activation energy. The excitation energy continuously vanishes with the longitudinal constraining field tending to zero. However, as discussed below, the half-metallicity imposes the restriction also on this type of fluctuations.

To study the longitudinal fluctuations of the Ni moments we impose the constraining field on the Ni atoms. Because of the interatomic hybridization the modification of the crystal states by the constraint is not restricted to the Ni sublattice. If the value of the Ni moment is determined by the constraint the variation of the moments of other atoms depends on the complex pattern of the interatomic hybridizations and usually cannot be predicted without concrete calculations. In half-metals such a prediction is possible.

First we consider the longitudinal constraint in a collinear magnetic configuration. To formulate the restriction imposed by the half-metallicity we note that the half-metallicity is not immediately destroyed by the application of the constraining field but must be preserved for a certain interval of the values of the field. The stability of the half-metallicity is determined by two factors: (i) The longitudinal constraint in the collinear magnetic configuration does not mix the states with opposite spin projections. The spin projection on the global spin-quantization axis remains a good quantum number and the spin-up and spin-down subsystems can be considered separately. (ii) The change in the electronic structure is continuous with the continuous variation of the constraining field h.[15]

The following scenario is expected. The change in the electronic structure caused by the constraining field will influence both the value of the semiconducting gap and the position of the Fermi level. At some critical values of the field the Fermi level reaches either the top of the valence band or the bottom of the conduction band and the half-metallic state becomes a normal metallic state. As long as the constraining field does not reach a critical value the magnetic moment per unit cell preserves its integer value and remains unchanged. As a result the change in the moment of one of the sublattices must be exactly compensated by the changes in the moments of other sublattices.

Turning from general consideration to the calculations for NiMnSb we first discuss the character of the changes in the DOS of the collinear magnetic configuration under the application of the constraining field. All calculations are performed with the augmented spherical wave (ASW) method[16] as described in our previous publications (see Refs. 14 and 17).

The ground-state values of the atomic moments are $m_{\mathrm{Ni}}=0.20\mu_B$, $m_{\mathrm{Mn}}=3.85\mu_B$, and $m_{\mathrm{Sb}}=-0.10\mu_B$. There is also

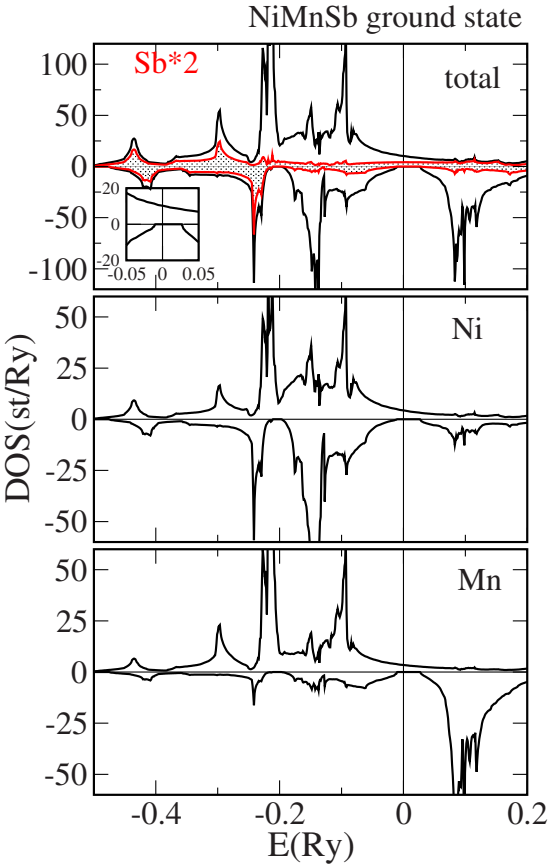

FIG. 1. (Color online) The ground-state DOS of NiMnSb. The upper panel shows the total DOS per formula unit and partial Sb DOS per atom. The Sb DOS is presented by the filled curve and is multiplied by factor 2 for better visualization. The inset shows the total DOS in the energy region around the Fermi level. The two lower panels present the partial Ni and Mn DOS.

small contribution coming from the empty sphere. The total moment per chemical formula is exactly $4\mu_B$. In Figs. 1 and 2 we present the total and partial DOS for the ground state and for the state with the constraining field $h=-25$ mRy corresponding to small Ni moment of $0.01\mu_B$.

The general structure of the DOS is similar in both cases. A closer inspection reveals, however, considerable differences. In the spin-up channel there are distinct changes in the structure of the peaks in the energy interval of the length of 0.2 Ry just below the Fermi level. On the other hand, the spin-down DOS preserves mostly the ground-state peak structure and differs by an energy shift with respect to the Fermi level. The semiconducting gap in the spin-down channel decreased somewhat and the Fermi level is now at the upper edge of the gap.

The properties of the gap in the spin-down channel for different values of the constrained Ni moment are summarized in Fig. 3 where the lower and upper boundaries of the gap are shown. The energy origin is for all calculations at the corresponding Fermi level. The gap is present for all values of the constrained Ni moment studied. The position of the gap with respect to the Fermi level varies continuously. For Ni moments larger than the ground state $m_{gr}=0.2\mu_B$ the Fermi level moves to the lower-energy part of the gap. At the

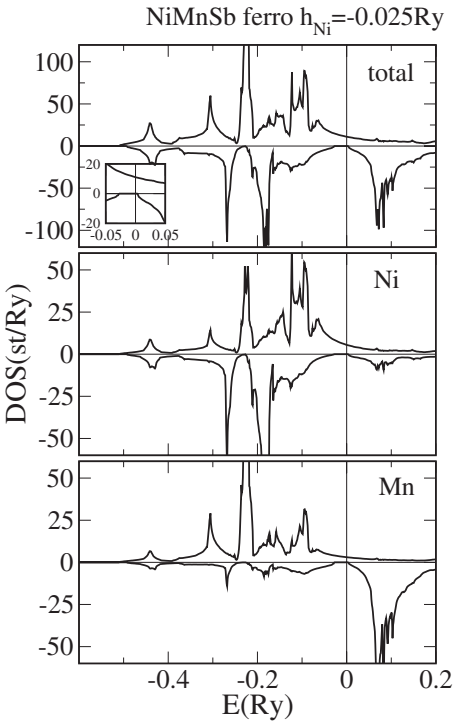

FIG. 2. The DOS for the collinear magnetic structure and the constraining field on Ni equal to −0.025 Ry. The presentation of the DOS is similar to Fig. 1.

moment of about $0.3\mu_B$ it reaches the top of the valence band and at the moment of about $0.07\mu_B$ the bottom of the conduction band. Outside of this interval the half-metallicity is destroyed and the system is in a normal metallic state. These results show that the half-metallicity is rather robust with respect to the longitudinal fluctuations of the Ni moments in the collinear magnetic configuration.

Figure 4 presents the changes in Mn and Sn moments caused by the constraint imposed on the Ni atom. Also the variation of the total moment per unit cell is given. As expected the change in the Ni moment is exactly compensated by the change in the moment of the rest of the unit cell in the interval of the variation of the Ni moment that preserves the

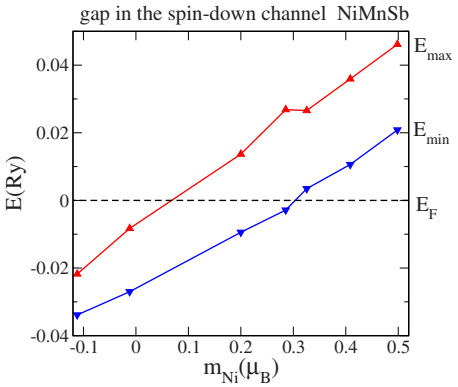

FIG. 3. (Color online) The upper and lower boundaries of the energy gap in the spin-down channel of energy structure of collinear magnetic configuration in NiMnSb as a function of the constrained Ni moment. The energy origin is at the Fermi level.

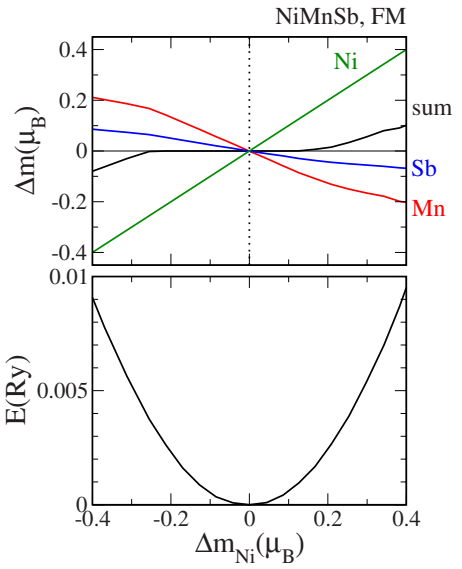

FIG. 4. (Color online) Upper panel: The change in the Mn and Sb atomic moments as well as the change in the total moment as a function of the change in the constrained Ni moment. Lower panel: The corresponding change in the total energy per formula unit.

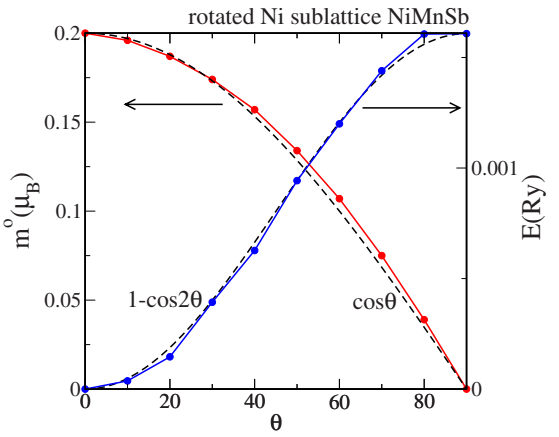

FIG. 5. (Color online) The m^0_{Ni} as a function of angle θ between Ni moments and the global z axis (left side axis) and the energy of the corresponding magnetic configurations (right side axis). The broken curves show scaled cos θ and $[1-\cos(2\theta)]$.

half-metallicity (Fig. 3). Beyond this interval the total moment begins to vary increasing or decreasing in accordance with the change in the Ni moment.

In the lower panel of Fig. 4 the energy as a function of the Ni moment is shown. The curve is rather symmetric with respect to the sign of the deviation of the moment from the ground-state value and is well described by a parabola. The energy obtained by constraining the Ni moment includes the contributions related to the change in the moments of other atoms caused by the hybridization of the atomic states.

There is an important aspect of the longitudinal fluctuations that is worth emphasizing here. Figure 4 shows that the intuitive relation between the values of the inducing and induced moments violates in the half-metallic systems. Indeed, the increase in the induced Ni moment leads to the decrease in the inducing Mn moment and vice versa. The same property was obtained by constraining the Mn moment and analyzing the change in the value of the Ni moment (not shown in this paper). This contraintuitive relation between induced and inducing moments appears in NiMnSb as a direct consequence of the half-metallicity. A similar property has, however, been obtained also in non-half-metallic systems like FeRh and reflects the complexity of the hybridization in magnetic multisublattice systems.[18]

Up to now we considered the longitudinal fluctuations of the Ni moments in the collinear ferromagnetic configuration. In the study of the thermal processes it is important to take into account the transversal fluctuations of the Ni moments. We performed calculations for the magnetic configurations with the Ni moments, keeping parallel directions with respect to each other, and rotated by angle θ relative to the global z axis. In these calculations the directions of the moments of the rest of the unit cell are kept parallel to the global z axis. In Fig. 5 we show the self-consistent Ni moment m^0_{Ni} as a function of angle θ. The value of the Ni moment decreases with increasing θ and vanishes at $\theta=90°$. This dependence is well described by the function $m^0_{\mathrm{Ni}}(\theta) = m_{\mathrm{gr}} \cos\theta$. There is no self-consistent state with the direction of the Ni moments forming the angle $\theta>90°$ with the Mn moments. In the calculations for $\theta>90°$ the Ni moment reverses the sign and converges to the state with $\theta'=180° - \theta$ that belongs to the angular interval from 0 to 90°. The calculated θ dependence of the energies of the self-consistent states is well described by the expression

$$E_{\mathrm{tr}}(\theta) = c[1-\cos(2\theta)], \tag{2}$$

with $c=0.804$ mRy.

Next we consider the variation of the spin polarization of the states at the Fermi level as a function of angle θ. As mentioned above for a noncollinear orientation of the Ni and Mn moments the spin projection of the electron states is not a good quantum number. Therefore any state has both spin-up and spin-down contributions that makes the 100% spin polarization not possible. The two-component spinor function has the form $\binom{\psi_1(\mathbf{r})}{\psi_2(\mathbf{r})}$ and the relation between the spin components varies from one space point to another. The same spinor state written with respect to different quantization axis is obtained by the transformation

$$\mathbf{U}(\theta)\begin{pmatrix}\psi_1(\mathbf{r})\\ \psi_2(\mathbf{r})\end{pmatrix}, \tag{3}$$

with spin-$\frac{1}{2}$ rotation matrix

$$\mathbf{U}(\theta) = \begin{pmatrix}\cos(\theta/2) & \sin(\theta/2)\\ -\sin(\theta/2) & \cos(\theta/2)\end{pmatrix}, \tag{4}$$

where the angle θ specifies the direction of the new quantization axis with respect to the old one. Obviously the spin polarization P given by

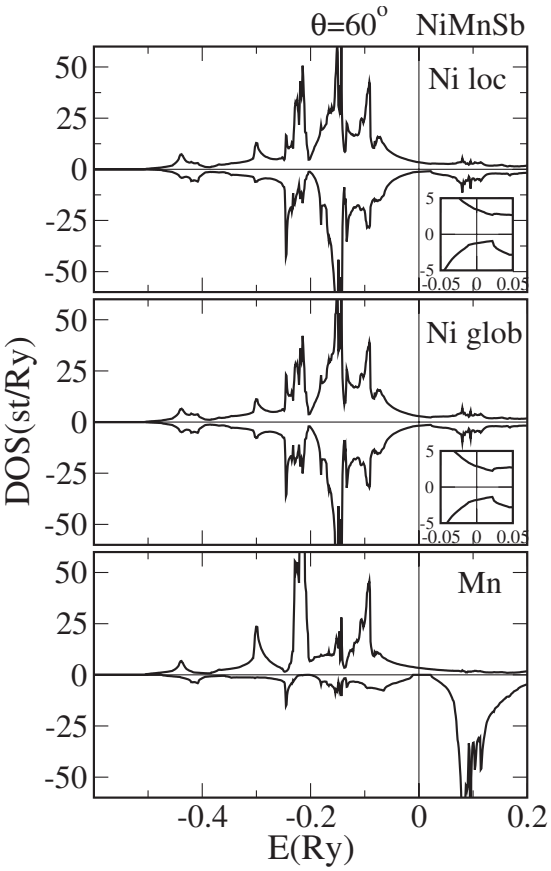

FIG. 6. The DOS of NiMnSb for the deviation of the Ni moments by θ=60°. Upper panel: The Ni DOS in the local spin frame. Middle panel: The Ni DOS in the global spin frame. Lower panel: The Mn DOS. The insets show the region close to the Fermi level.

$$P = \frac{\psi_1^2 - \psi_2^2}{\psi_1^2 + \psi_2^2} \tag{5}$$

is not invariant with respect to the change in the quantization axis.

Two types of axes are physically most important: the global z axis parallel to the direction of the net magnetization of the system and local atomic axes parallel to the directions of the atomic moments. The spin polarization with respect to the local atomic axis shows how well the spin of the electron state adjusts itself to the exchange field of the atom. On the other hand, the spin polarization with respect to the global axis is important for the spintronic applications since the global axis is used to register and manipulate the spin.

In Fig. 6 we present the partial Ni and Mn DOS for the case of θ=60°. The value of the Ni moment is in this case m_{Ni}=0.11μ_B. For the Ni atom, the densities are calculated with respect to both local and global quantization axes. The Mn DOS resembles the Mn DOS in the ferromagnetic case (Fig. 1). The two spin components of the Mn DOS are again very different. The majority-spin Mn 3d states lie mostly below the Fermi level whereas the minority-spin Mn 3d states are mostly above the Fermi level. The spin polarization of the Mn states at the Fermi energy is close to 100%.

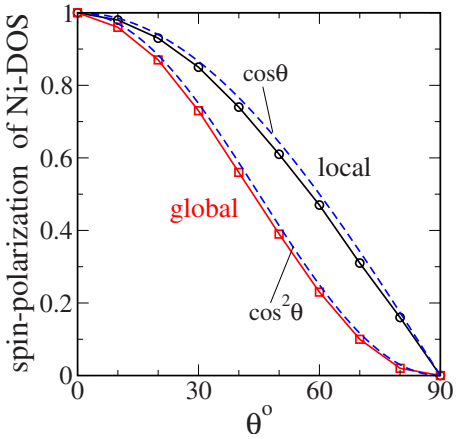

FIG. 7. (Color online) The spin polarization of the Ni DOS at the Fermi level. The polarization is calculated in both global and local spin-coordinate systems. The broken curves show cos θ and cos^2 θ functions that well describe the form of the polarization in both frames of references.

For the Ni atoms, the situation is different. Already in the local system the spin-up and spin-down DOS are closer to each other than in the ferromagnetic case (Fig. 1). This reflects the property that both spin components are now the parts of the same states since the spin projection is not a good quantum number. The spin polarization at the Fermi level deviates strongly from 100% and assumes the value of 47%. In the global spin-coordinate system the similarity between both spin components of the Ni DOS increases further. Simultaneously the spin polarization of the Ni DOS at the Fermi level decreases to 23%.

In Fig. 7 we present the spin polarization of the Ni DOS at the Fermi energy as a function of angle θ. The fast decrease in the spin polarization of the partial Ni DOS with increasing θ reveals that thermal fluctuations of the Ni moments can be the origin of the strong decrease in the spin polarization of the corresponding part of the electron state. The θ dependence of the spin polarization with respect to the local quantization axis is close to cos θ and therefore follows the θ dependence of the local Ni moment m_{Ni}^0 (Fig. 5). The spin polarization with respect to the global quantization axis is close to cos^2 θ that gives the projection of the local Ni moment on the global z axis.

Next we turn to the longitudinal fluctuations of the Ni moments in the noncollinear configurations. In Figs. 8 and 9 we show the results of the calculations of the longitudinal Ni constraint for θ=30° and θ=90° similar to the calculations shown in Fig. 4 for the collinear configuration. The results for θ=30° resemble in main features the results in Fig. 4. However, the compensation of the changes in different atomic moments is here not perfect and the sum of the moments decreases or increases together with the Ni moment although much slower.

For θ=90° the situation is very different and the change in the Ni moment does not lead to the change in the moments of other sublattices (Fig. 9). Comparison of the energy curves shows that the coefficient of the parabola describing the energetics of the longitudinal fluctuations decreases somewhat with increasing θ. In the statistical model studied

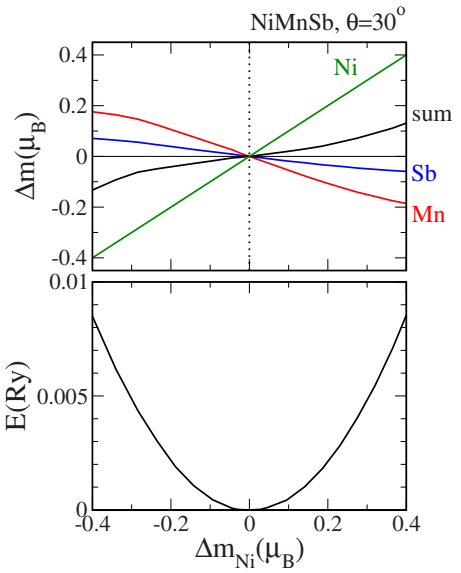

FIG. 8. (Color online) Upper panel: The change in the Mn and Sb atomic moments as well as the change in the sum of the atomic moments as a function of the change in the constrained Ni moment. The calculations are performed for $\theta=30°$. Lower panel: The corresponding change in the total energy per formula unit.

below we will neglect this difference and use the same longitudinal stiffness $a=58.6$ mRy/μ_B^2 for all θ. The energies in Figs. 4, 8, and 9 are counted from the energies of the states corresponding to $m_{\mathrm{Ni}}^0(\theta)$ giving the minimum of the energy for corresponding θ. The position of this minimum increases with θ (Fig. 5).

The longitudinal constraint leads to the change in the spin polarization of the states at the Fermi level compared to the polarization of the m_{Ni}^0 state shown in Fig. 7. Here we do not present the corresponding data. Below in the discussion of the temperature dependence of the polarization we show the polarizations calculated for values corresponding to the thermal averages of the Ni moment.

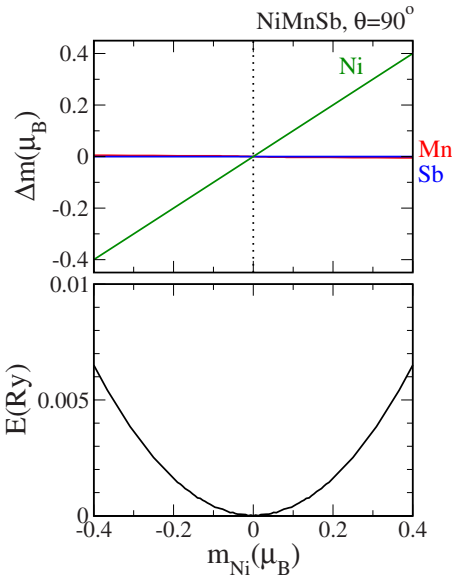

FIG. 9. (Color online) Upper panel: The change in the Mn and Sb atomic moments as well as the change in the sum of the atomic moments as a function of the change in the constrained Ni moment. The calculations are performed for $\theta=90°$. Lower panel: The corresponding change in the total energy per formula unit.

IV. STATISTICAL MECHANICS MODEL

A. Description of the model

As stated above we study the temperature interval where the disordering in the Mn sublattice is weak and can be neglected. The main temperature effects are expected to come from the thermal properties of the Ni sublattice. The possible scenarios in the magnetic temperature behavior of the Ni sublattice are, for example, the collapse of the atomic Ni moments, the decoupling of the Ni moments from the Mn moments or, opposite, a strong connection between the temperature dependencies of the net magnetizations of the Ni and Mn sublattices. Our previous studies of NiMnSb have shown that Ni-Ni exchange interaction is weak.[17] This allows us to consider one fluctuating Ni moment. The states of the Ni moment are determined by angle θ with respect to the global z axis and the value of the Ni moment m. The energy of the state (θ,m) is given by

$$E(\theta,m) = E_{\mathrm{tr}}(\theta) + E_{\mathrm{long}}(\theta,m), \tag{6}$$

where $E_{\mathrm{tr}}(\theta)$ is defined above and

$$E_{\mathrm{long}}(\theta,m) = a[m - m^0(\theta)]^2 = a(m - m_{\mathrm{gr}}\cos\theta)^2, \tag{7}$$

with $a=58.6$ mRy/μ_B^2.

The partition sum of the model has the form

$$Z = \int_0^{2\pi} d\phi \int_0^{\frac{\pi}{2}} d\theta \sin\theta \int_{-\infty}^{\infty} dm m^2 \exp[-E(\theta,m)/k_BT]. \tag{8}$$

The energies are invariant with respect to angle ϕ. Therefore the integration over ϕ in Eq. (8) gives a trivial 2π factor. In the calculations of the average values of the physical quantities that do not depend on ϕ this factor cancels with the corresponding factor in the numerator.

An important feature of expression (8) is the Jacobian m^2 of the spherical coordinate system. It reflects the property that in the treatment of the atomic moments as three-dimensional vectors the statistical weight of the states with large length of the vector is larger than the statistical weight of the states with small length of the vector. There is no analog of this factor in the Heisenberg-type models where only the directions of the moments are considered as independent variables.

The average value of physical quantity $f(\theta,m)$ is given by

$$\langle f(\theta,m)\rangle = \frac{2\pi}{Z}\int_0^{\frac{\pi}{2}} d\theta \sin\theta \times \int_{-\infty}^{\infty} dm m^2 f(\theta,m)\exp[-E(\theta,m)/k_BT]. \tag{9}$$

In the calculation of the average value of the z projection of

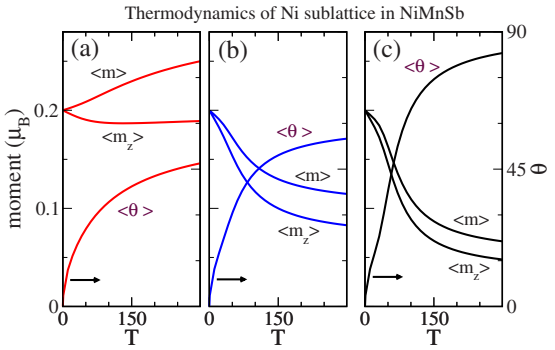

FIG. 10. (Color online) The thermodynamics of the Ni sublattice. Panel (a) presents calculation with full model [Eqs. (8) and (9)]. Panel (b) gives the results for the model with Jacobian m^2 neglected. The results in panel (c) are obtained with only the integration over the angular variables preserved. Shown are average magnetization $\langle m_z \rangle$, average atomic moment $\langle m \rangle$, and average angle $\langle \theta \rangle$ of the deviation from the z axis.

the Ni moments $\langle m_{\mathrm{Ni}}^z \rangle$ function $f(\theta,m)=m \cos\theta$ is used, the average values of the length of the Ni moment $\langle m_{\mathrm{Ni}} \rangle$ are obtained with $f(\theta,m)=m$, and the average cosine of θ is calculated with $f(\theta,m)=\cos\theta$.

B. Results and discussion

In Fig. 10 we present the calculated temperature dependence of the average magnetization of the Ni sublattice $\langle m_{\mathrm{Ni}}^z \rangle$, the average value of the Ni moment $\langle m_{\mathrm{Ni}} \rangle$, and the average angle $\langle \theta \rangle$ determined as $\arccos\langle \cos\theta \rangle$. The calculation with the model given by Eq. (8) shows that the net magnetic moment stabilizes after small decrease by about 5% in the first 50 K. The average length $\langle m_{\mathrm{Ni}} \rangle$ increases monotonously and assumes the values of $0.23\mu_B$ and $0.25\mu_B$ at 150 K and 300 K. The average angle $\langle \theta \rangle$ also increases monotonously and has the values of 39° and 47° at 150 K and 300 K. Thus the deviation of the Ni moment from the magnetization direction is considerable. Neither a collapse of the Ni moment nor substantial decrease in the net magnetization of the Ni sublattice is obtained. Such a behavior agrees with experimental temperature dependence of the total net magnetization of NiMnSb that does not show any specific features in the low-temperature region.

There are two experimental reports on the temperature dependence of the partial magnetization of the Ni atoms. Hordequin *et al.*[19] performed polarized neutron diffraction on NiMnSb and obtained $\langle m_{\mathrm{Ni}}^z \rangle = 0.18\mu_B$ at 15 K and $\langle m_{\mathrm{Ni}}^z \rangle = 0.19\mu_B$ at 260 K. This weak temperature dependence of the net Ni moment is in very good agreement with our calculations. On the other hand, the magnetic circular dichroism measurements by Borca *et al.*[4] are interpreted as giving about 50% drop of both Mn and Ni moments between 50 and 150 K. Such a behavior disagrees strongly with the temperature dependence of the total net magnetization. We hope that the present work will stimulate further magnetic circular dichroism studies of this system.

Figure 11 shows the probability distribution for the value of the Ni moment that increases strongly with temperature.

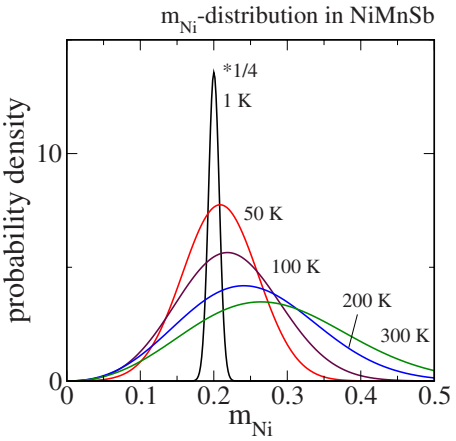

FIG. 11. (Color online) The probability density of the Ni magnetic moment for a number of temperatures.

For $T=200$ K the square root of the variance is 0.12. The average value of the moment at this temperature is 0.24. Therefore the relation of the average deviation from the average value to the average value is 50%. At $T=300$ K the average value increases to $0.25\mu_B$ and average deviation to 62% of this value.

To understand the role of the m^2 factor in the calculation of the thermodynamic averages we performed the calculations omitting this factor. Physically such a model means that the longitudinal fluctuations of a moment are considered separately for each direction of the moment. Therefore the statistical weight of the fluctuations does not change with the change of the length. Although the energy as a function of θ and m remains the same the temperature dependence of averages changes strongly [Fig. 10(b)]. We obtain strong decrease in $\langle m_z \rangle$ in the interval between 0 and 100 K. At $T=50$ K, the net magnetic moment is about 75% of the ground-state value. It decreases to 55% at 100 K. The further decrease becomes slower. At 150 K and 300 K the magnetization is, respectively, 50% and 41% of the ground-state value.

If we completely neglect the longitudinal fluctuations and take for each direction of the Ni moment only the state with the lowest energy corresponding to $m^0(\theta)$ the magnetization decreases even faster [Fig. 10(c)]. For example at $T=100$ K it has 44% of its value in the ground state. Also the increase in the average deviation angle $\langle \theta \rangle$ with temperature is maximal in this case.

Summarizing the analysis of Fig. 10 we conclude that, first, a consequent treatment of the longitudinal fluctuations of the Ni moments results in a very weak temperature dependence of the Ni magnetization in the temperature region where the Mn disordering can be neglected. This weak temperature dependence of the magnetization is not a result of a weakness of the magnetic fluctuations. At $T=100$ K the average deviation angle is 34°. The transversal fluctuations of the Ni moment are compensated by the fluctuations of the value of the moment to lead to almost constant value of the magnetization. If the Jacobian m^2 is neglected the compensation does not take place.

In Fig. 12 we compare the Ni DOS in the energy region around the Fermi level for the ground state ($\theta=0$ and m

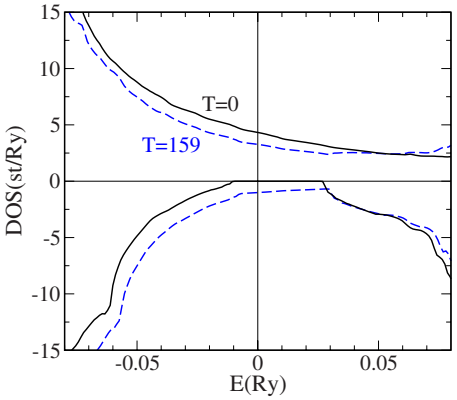

FIG. 12. (Color online) The spin-resolved Ni DOS in the ground state (solid line) and at $T=159$ K (broken line).

$=0.2\mu_B$) and for the state with $\theta=40°$ and $m=0.23\mu_B$ corresponding to the average angle and average moment at $T=159$ K. The spin projections of the DOS are given with respect to the global axis. In the main part of the energy interval the heating leads to the decrease in the spin-up DOS and the increase in the spin-down DOS. An opposite trend is obtained only for unoccupied states at energies above 0.05 Ry. The half-metallicity is disturbed: no gap remains in the spin-down DOS.

In Fig. 13 we present the spin polarization of the Ni DOS calculated for the configurations characterized by average values of angle $\langle\theta\rangle(T)$ and Ni atomic moment $\langle m_{\mathrm{Ni}}\rangle(T)$ for a number of temperatures. This result shows again that the decrease in the spin polarization begins immediately with the temperature rising above 0 K. An interesting feature of the calculated data is that indeed a kind of crossover in the temperature region between 75 and 100 K can be registered. The calculated values in two temperature intervals, below 75 K and above 100 K, are well described by straight lines. The coefficients of these curves are however different. At low temperatures the decrease in the magnetization per 1 K is larger than for higher temperatures. This crossover is a combined effect of different factors such as the temperature dependences of average magnetic moment $\langle m\rangle$, of average angle $\langle\theta\rangle$, the dependence of the features of the DOS on angle θ and moment m_{Ni}. We have shown that the longitudinal fluctuations contribute importantly to the formation of the averages and that the properties of the longitudinal fluctuations are strongly influenced by the half-metallicity of the ground state. Nevertheless the characterization of the cross-over in the temperature dependence of the polarization as a transition between the half-metallic and normal metallic state does not have a real physical basis since the half-metallicity is not preserved up to the cross-over temperature region. Therefore our calculation agrees with experiments reporting a crossover in the properties of NiMnSb at about 80 K. We argue that the crossover cannot be treated as the transition from half-metallic to non-half-metallic state. It reflects complex properties of the magnetic fluctuations in NiMnSb. The half-metallicity of the ground state is an important factor influencing the properties of the fluctuations.

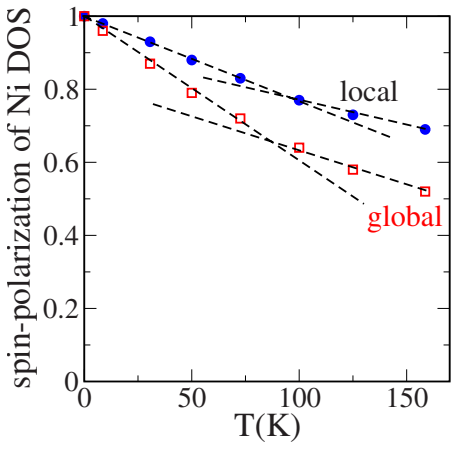

FIG. 13. (Color online) The spin polarization of the Ni DOS at the Fermi level as a function of temperature. The polarization is calculated in both global and local spin-coordinate systems.

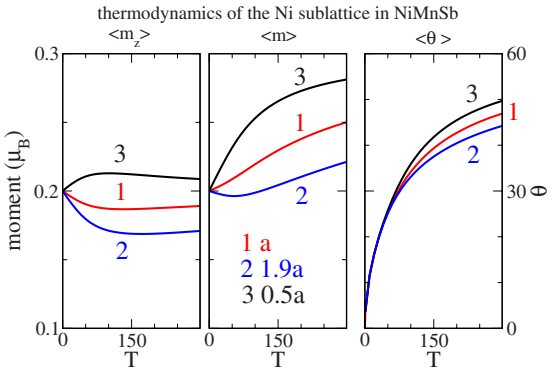

FIG. 14. (Color online) Temperature dependence of the average magnetization $\langle m_z\rangle$, average atomic moment $\langle m\rangle$, and average angle $\langle\theta\rangle$ of the deviation from the z axis for the Ni sublattice. The calculations are performed for three different values of the longitudinal stiffness of the Ni moment: a, $0.5a$, $1.9a$.

C. Variation of the longitudinal stiffness

As follows from the discussion above a natural treatment of the thermodynamics of itinerant-electron magnets is the mapping of the system on a **m**-type model that takes into account the fluctuations of both the direction and the length of the magnetization. Since the use of the Heisenberg-type Hamiltonian is substantially simpler it is very often used in the studies of the thermodynamics of magnetic systems. In the Appendix we discuss the conditions that allow to reduce the consideration from **m**-type model to **e**-type model.

An important condition for such a reduction is a large value of the longitudinal stiffness that satisfies the inequality $a \gg kT$. In this context it is instructive to see how strong is the dependence of the thermal averages shown in Fig. 10(a) on the value of the exchange stiffness. We performed additional calculations with parameters of the longitudinal stiffness $a'=1.9a$ and $a''=0.5a$, where a is the stiffness used above. The results of the calculations are presented in Fig. 14 and reveal substantial dependence on the value of the stiffness. Both $\langle m_z\rangle$ and $\langle m\rangle$ compared at the same temperature assume larger values for smaller stiffnesses. The decrease in

the stiffness leads to the decrease in the energy of the longitudinal fluctuations of magnetization. The energy curve in the form of parabola is symmetric with respect to the minimum. Therefore the change in the stiffness influences in the same way the Boltzmann factor to the right and to the left of the minimum point making larger fluctuations more probable. The balance between two directions of the fluctuations is disturbed by the Jacobian m^2 increasing the statistical weight of larger m values.

The strong dependence on the value of a shows that even for rather high values of the longitudinal stiffness the longitudinal fluctuations make significant contribution to thermodynamics. We do not present the results of the variation of parameter c responsible for the θ dependence of the energy minimum corresponding to m_0 (Fig. 5). There is a simple scaling relation that the average values for temperature T and parameters $(\alpha a, c)$ equal to the averages for temperature $\frac{T}{\alpha}$ and parameters $(a, \frac{c}{\alpha})$.

D. Closing remarks on the theoretical scheme

Closing the discussion of the thermodynamic model suggested in the paper we emphasize two important features of the calculational scheme. First, the parametrization of the energy of magnetic fluctuations includes explicitly (i) the calculated values of the magnetic moments supplying the minima of the total energy for different relative orientations of the Ni and Mn atomic moments and (ii) the calculated longitudinal stiffnesses of the moments for these orientations. The second feature is a consequent treatment of the Jacobian m^2 in the evaluation of the statistical weight of magnetic states.

To the author's knowledge there are two earlier DFT-based studies of the thermodynamics of NiMnSb that take longitudinal fluctuations of the atomic moments into account. The work of Kübler[20] focuses on the calculation of the Curie temperature. It studies the fluctuations of the Mn moments and does not consider the fluctuations of the Ni moment that are the main subjects of the present study. Ležaić *et al.*[6] use substantially different parametrization of the energy of the fluctuations of the Ni moments. For the ith Ni moment the energy is written in the form

$$am_i^2 + bm_i^4 - \left(\sum_{j\neq i} J_{ij}\mathbf{m_j}\right)\mathbf{m_i}, \tag{10}$$

where J_{ij} are Heisenberg exchange parameters and sum over j includes summation over Mn and Ni moments. All coefficients a, b and J_{ij} are constant and do not depend on the magnetic configuration. Considering the longitudinal fluctuation of the ith moment along a specified direction $\mathbf{e}_i$ expression (10) allows determining both the value of the moment m_i^0 corresponding to the minimum of the energy and the longitudinal stiffness of the moment determined by the second derivative with respect to m_i at the point of minimum. Variation of $\mathbf{e}_i$ results in a correlated change in both m_i^0 and stiffness governed by the values of the configuration-independent parameters a, b and J_{ij}. This parametrization differs considerably from the scheme used in the present paper where the values of m_i^0 and stiffness are determined in direct DFT calculations for various magnetic configurations. The difference in the energy parametrization may be the reason for the difference in the low-temperature thermodynamics of the Ni moments obtained in the two works.

Note that the extension of the approach suggested in the paper to the consideration of the model that treats on an equal footing the thermodynamics of Ni, Mn, and Sb sublattices is desirable and constitutes an interesting problem for future studies. Such an extension is necessary to study the thermal properties of NiMnSb up to and above the Curie temperature.

It is also worth mentioning that the account for the electron correlations on the Mn sites performed within the dynamical mean-field theory (DMFT) (Ref. 2) points out on the formation of the nonquasiparticle states (NQPS) above the Fermi level in the semiconducting spin-down channel. To the author's knowledge the influence of the NQPS on the thermodynamics of the Ni sublattice has not yet been studied.

V. CONCLUSIONS

We report a detailed theoretical study of the thermal magnetic properties of the Ni sublattice in half-metallic NiMnSb. The study is performed in the temperature interval where the disordering of the Mn sublattice is weak and the properties of the Ni sublattice can play a crucial role. In earlier work it was suggested that the behavior of the Ni sublattice is responsible for the anomalies in the properties of NiMnSb detected experimentally at about 80 K. We formulate a thermodynamic model where both transversal and longitudinal fluctuations of the magnetic moments are taken into account. We show that the half-metallicity is robust with respect to the longitudinal atomic fluctuations in the ground-state ferromagnetic structure. On the other hand the half-metallicity imposes strong restrictions on the longitudinal fluctuations. In contrast to longitudinal fluctuations the transversal fluctuations disturb the half-metallicity. We show that the contributions of the longitudinal and transversal fluctuations to the temperature dependence of the Ni net magnetization compensate, which leads to a very weak variation of the Ni magnetization in a broad temperature interval. This feature is in agreement with experiment. Simultaneously a large amplitude of the fluctuations results in strong decrease in the spin polarization of the Ni DOS at the Fermi level. The calculated temperature dependence of the Ni spin polarization reveals a crossover in the temperature interval between 75 and 100 K that correlates with experimental features in the temperature dependences of the physical properties. Although this crossover cannot be interpreted as the transition from a half-metallic to a non-half-metallic state the half-metallicity of the ground state is an important factor determining the properties of the fluctuations and the temperature properties.

Since at room temperature the magnetic disorder of the Ni sublattice is stronger than the disorder of the Mn sublattice the spin polarization of the partial Ni density of states is much weaker than the spin polarization of the Mn density of states. Therefore in the fabrication of the devices aiming the injection of spin-polarized electrons from NiMnSb to a semiconductor the termination of NiMnSb at the interface

NiMnSb semiconductor with the layer of Mn atoms can result in much better injection performance than the termination with Ni layer. An experimental verification of the relation between the temperature dependence of the spin-injection process and the termination of the magnetic system at the interface with semiconductor is desirable.

ACKNOWLEDGMENTS

The author acknowledges interesting discussions with Phivos Mavropoulos, Marjana Ležaić, Stefan Blügel, Björn Alling, Marcus Ekholm, and Igor Abrikosov.

APPENDIX: HEISENBERG-TYPE MODEL AS A LIMIT OF THE m MODEL

In this section we discuss within the concepts used in this paper the physical limit in which the consideration of the **m**-type model can be reduced to the consideration of the **e**-type model.

We start with the expression for the energy that is the generalization of Eqs. (6) and (7)):

$$E(\{\mathbf{m}_i\}) = E_{\mathrm{tr}}(\{\mathbf{e}_i\}) + \sum_i a_i[m_i - m_i^0(\{\mathbf{e}_i\})]^2. \tag{A1}$$

Here $=E_{\mathrm{tr}}(\{\mathbf{e}_i\})$ is the lowest energy for the states with spin-configuration $(\{\mathbf{e}_i\})$ and $m_i^0(\{\mathbf{e}_i\})$ is the corresponding set of the values of the magnetic moments. The second term in Eq. (A1) describes the energy of the longitudinal fluctuations. The partition function is given by

$$Z = \prod_j \int dm_j m_j^2 \exp[-\beta a_j (m_j - m_j^0(\{\mathbf{e}_i\}))^2] \times \int\int \prod_i d\phi_i d\theta_i \sin\theta_i \exp[-\beta E(\{\mathbf{e}_i\})], \tag{A2}$$

where $\beta = 1/k_B T$. The average magnetization is given by

$$\langle m_z \rangle = \sum_i \frac{\int dm_i m_i^3 \exp(-\alpha_i\{m_i - m_i^0[(\mathbf{e}_i)]\}^2)}{\int dm_i m_i^2 \exp(-\alpha_i\{m_i - m_i^0[(\mathbf{e}_i)]\}^2)} \times \int\int \prod_{j\neq i} d\phi_j d\theta_j \sin\theta_j \times \int\int d\phi_i d\theta_i \sin\theta_i \cos\theta_i \exp\{-\beta E[(\mathbf{e}_i)]\} \times \left(\int\int \prod_i d\phi_i d\theta_i \sin\theta_i \exp\{-\beta E[(\mathbf{e}_i)]\}\right)^{-1}, \tag{A3}$$

where $\alpha_i = a_i/k_B T$.

The mapping of a given system on a Heisenberg-type Hamiltonian is valid in the case that the integrations in Eq. (A3) can be reduced to the integration over angular variables only. It can be verified that if $m_i^0(\{\mathbf{e}_i\})$ does not depend on $\{\mathbf{e}_i\}$ and the longitudinal stiffnesses satisfy the condition $a_i \gg kT$ the expression for the average magnetization indeed takes a Heisenberg-type form,

$$\langle m_z \rangle = \sum_i m_i^0 \int\int \prod_{j\neq i} d\phi_j d\theta_j \sin\theta_j \times \int\int d\phi_i d\theta_i \sin\theta_i \cos\theta_i \exp[-\beta E(\{\mathbf{e}_i\})] \times \left(\int\int \prod_i d\phi_i d\theta_i \sin\theta_i \exp[-\beta E(\{\mathbf{e}_i\})]\right)^{-1}. \tag{A4}$$

If $m_i^0(\{\mathbf{e}_i\})$ depends on $\{\mathbf{e}_i\}$ expression (A3) does not reduce to the Heisenberg-type form even if the longitudinal stiffnesses $a_i \gg kT$. The Jacobian m^2 entering the general formula (A3) leads to additional terms in the angular dependence of the integrand function. If the condition $a_i \gg kT$ on the longitudinal stiffness is not fulfilled the integration over the values of the moments gives non-negligible contribution into configurational integral.

*lsandr@mpi-halle.de

[1] R. A. de Groot, F. M. Mueller, P. G. van Engen, and K. H. J. Buschow, Phys. Rev. Lett. **50**, 2024 (1983).
[2] M. I. Katsnelson, V. Yu. Irkhin, L. Chioncel, A. I. Lichtenstein, and R. A. de Groot, Rev. Mod. Phys. **80**, 315 (2008).
[3] C. Hordequin, D. Ristoiu, L. Ranno, and J. Pierre, Eur. Phys. J. B **16**, 287 (2000).
[4] C. N. Borca, T. Komesu, H.-K. Jeong, P. A. Dowben, D. Ristoiu, C. Hordequin, J. P. Nozieres, J. Pierre, S. Stadler, and Y. U. Idzerda, Phys. Rev. B **64**, 052409 (2001).
[5] M. J. Otto, R. A. van Woerden, P. J. van der Valk, J. Wijngaard, C. F. van Bruggen, C. Haas, and K. H. J. Buschow, J. Phys.: Condens. Matter **1**, 2341 (1989).
[6] M. Ležaić, Ph. Mavropoulos, J. Enkovaara, G. Bihlmayer, and S. Blügel, Phys. Rev. Lett. **97**, 026404 (2006).
[7] J. J. Attema, G. A. de Wijs, and R. A. de Groot, J. Phys.: Condens. Matter **19**, 315212 (2007).
[8] N. D. Mermin, Phys. Rev. **137**, A1441 (1965).
[9] J. Kübler, *Theory of Itinerant Electron Magnetism* (Clarendon, Oxford, 2000).
[10] B. L. Gyorffy, A. J. Pindor, J. Staunton, G. M. Stocks, and H. Winter, J. Phys. F: Met. Phys. **15**, 1337 (1985).
[11] P. H. Dederichs, S. Blügel, R. Zeller, and H. Akai, Phys. Rev. Lett. **53**, 2512 (1984).
[12] V. Antropov, Phys. Rev. B **72**, 140406(R) (2005).
[13] A. V. Ruban, S. Khmelevskyi, P. Mohn, and B. Johansson, Phys. Rev. B **75**, 054402 (2007).
[14] L. M. Sandratskii, R. Singer, and E. Şaşıoğlu, Phys. Rev. B **76**,

184406 (2007).

[15] Here we exclude from the consideration the possible instability of the system with respect to a discontinuous transition to a new state under the influence of the constraining field. Such transition is in principle possible if the energy as a function of the value of the magnetic moment has several minima corresponding to the low-spin and high-spin states of the material. This situation does not realize in NiMnSb.

[16] A. R. Williams, J. Kübler, and C. D. Gelatt, Phys. Rev. B **19**, 6094 (1979).

[17] E. Şaşıoğlu, L. M. Sandratskii, P. Bruno, and I. Galanakis, Phys. Rev. B **72**, 184415 (2005).

[18] L. M. Sandratskii (unpublished).

[19] Ch. Hordequin, E. Lerievre-Berna, and J. Pierre, Physica B (Amsterdam) **234-236**, 602 (1997).

[20] J. Kübler, Phys. Rev. B **67**, 220403(R) (2003).